836 *Inorg. Chem.* **2011**, *50*, 836–846
DOI: 10.1021/ic101350f

Inorganic Chemistry
Article

Effect of Inclining Strain on the Crystal Lattice along an Extended Series of Lanthanide Hydroxysulfates Ln(OH)SO_4 (Ln = Pr−Yb, except Pm)

Ralph A. Zehnder,*,† Christopher S. Wilson,‡ Hunter T. Christy,‡ Kenneth S. Harris,† Varun Chauhan,† Victor Schutz,† Matthew Sullivan,† Matthias Zeller,§ Frank R. Fronczek,∥ Jacob A. Myers,† Kyle Dammann,‡ James Duck,‡ Peter M. Smith,⊥ Antony Okuma,§ Kristin Johnson,§ Robert Sovesky,§ Cameron Stroudt,† and Robert A. Renn‡

†*Department of Chemistry, and* ‡*Department of Biology, University of Louisiana at Monroe, Monroe, Louisiana 71209, United States,* §*Department of Chemistry, Youngstown State University, Youngstown, Ohio 44555, United States,* ∥*Department of Chemistry, Louisiana State University, Baton Rouge, Louisiana 70803, United States, and* ⊥*Department of Chemistry, Westminster College, New Wilmington, Pennsylvania 16172, United States*

Received July 7, 2010

A series of trivalent lanthanide hydroxysulfates, Ln(OH)SO_4, (Ln = Pr through Yb, except radioactive Pm) has been synthesized via hydrothermal methods from $Ln_2(SO_4)_3 \cdot 8H_2O$ by reaction with aqueous NaOH at 170 °C in Teflon lined Parr steel autoclaves, and were characterized by single crystal X-ray diffraction and FT-IR spectroscopy. Two types of arrangements were found in the solid state. The lighter (Ln = Pr−Nd, Sm−Gd) and heavier lanthanide(III) hydroxysulfates (Tb−Yb) are each isostructural. Both structure types exhibit the monoclinic space group $P2_1/n$, but the unit cell content is doubled with two crystallographically distinct LnO_8 polyhedra for the heavier lanthanide compounds. The lighter complexes maintain the coordination number 9, forming a three-dimensional extended lattice. The heavier counterparts exhibit the coordination number 8, and arrange as infinite columns of two crystallographically different LnO_8 polyhedra, while extending along the "*c*" axis. These columns of LnO_8 polyhedra are surrounded and separated by six columns of sulfate ions, also elongating in the "c" direction. The rigid sulfate entities seem to obstruct the closing in of the lighter LnO_9 polyhedra, and show an inclining degree of torsion into the "*ac*" layers. The crystal lattice of the lighter 4f complexes can sufficiently withstand the tension buildup, caused by the decreasing Ln^{3+} radius, up to Gd(OH)SO_4. The energy profile of this structural arrangement then seems to exceed levels at which this structure type is favorable. The lattice arrangement of the heavier Ln-analogues seems to offer a lower energy profile. This appears to be the preferred arrangement for the heavier lanthanide hydroxysulfates, whose crystal lattice exhibits more flexibility, as the coordination sphere of these analogues is less crowded. The IR absorbance frequencies of the hydroxide ligands correlate as a function of the Ln^{3+} ionic radius. This corresponds well with the X-ray single crystal analysis data.

Introduction

Extended series of lanthanide compounds are useful for examining the effects of the decreasing ionic radius on the crystal lattice with increasing atomic numbers. Some lanthanide compounds exhibit identical coordination numbers and similar structural parameters for their lighter and heavier analogues. Others undergo phase transitions and/or adjust structural parameters to compensate for the increasing strain placed on the crystal lattice for the heavier lanthanide compounds because of smaller ionic radii.[1,2] Generally, with the decreasing ionic radius along a series of similar lanthanide compounds, the space for coordination is reduced and, as a result, coordination numbers vary from nine to eight to six in some instances.[3] Because of their similarities with the actinides, in regard to ionic radius and covalence, lanthanide compounds can be utilized as surrogates for corresponding radioactive actinide compounds.

Related actinide(III) complexes can be prepared utilizing analogous methods, and their structural and physicochemical properties often compare well.[4]

Thus, the detailed study of series of lanthanide mixed ligand complexes is expected to lay the groundwork for the creation and characterization of corresponding actinide analogues.

*To whom correspondence should be addressed. Phone: (+1)318-342-1836. E-mail: zehnder@ulm.edu. Fax (+1)318-342-3334.

(1) Haschke, J. M. Halides. In *Handbook on the Physics and Chemistry of Rare Earths*; Elsevier North-Holland: Amsterdam, The Netherlands, 1979; Vol. *4*, pp 89−151.

(2) Wickleder, M. S. *Chem. Rev.* **2002**, *102*, 2011–2087.

(3) Kaltsoyannis, N. *The f elements*; Oxford University Press: Oxford, 1999; Giesber, H.; Ballato, J.; Chumanov, G.; Kolis, J.; Dejneka, M. *J. Appl. Phys.* **2003**, *93*(11), 8987–8994.

 Published on Web 01/05/2011

This may bear important implications for the sequestering and subsequent storage of nuclear waste materials.

Recently we reported how the crystal lattice responds to tension buildup, caused by the decreasing ionic radius within an extended series of lanthanide bis-hydroxychlorides, ($Ln(OH)_2Cl$).[5] In this work we continue our efforts aiming at the creation of extended series of purely inorganic lanthanide mixed ligand complexes with a focus on the elucidation and comparison of their structural trends. In our previous manuscript we pointed out that the metal centers throughout the extended series of $Ln(OH)_2Cl$ consistently display the coordination number 8. Apparently the crystal lattice responds to the increasing strain resulting from the shortening of the ionic radius for the heavier analogues via certain adjustments of unit cell and lattice parameters that are specifically associated with the crystallographic "*a* axis".[5] The motivation behind this work was to answer the question if similar effects can be observed for the lanthanide hydroxysulfates ($Ln(OH)SO_4$), or if a phase transition can be observed going along with a change in coordination numbers. In case of such a phase transition we were hoping to locate this "break" in the crystal lattice. Herein we illustrate that the structural trends within this series of lanthanide hydroxysulfates are in great contrast to the lanthanide bis-hydroxychlorides. The direct comparison of the structural properties as a function of the decreasing ionic radius from the lighter to the heavier lanthanides in these two series appears to be quite fascinating.

We obtained X-ray quality single crystals of the lanthanide hydroxysulfates by applying a very similar hydrothermal synthetic methodology as compared to the synthesis of lanthanide bis-hydroxychlorides. For the creation of lanthanide hydroxysulfates we applied somewhat lower reaction temperatures. [Lower reaction temperatures significantly decrease the thermal wear of the Teflon lined Parr steel autoclaves, resulting in a considerable increase of the equipment's lifespan.]

A few lanthanide hydroxysulfates have been previously structurally determined via single crystal X-ray analysis by various researchers. $Eu(OH)SO_4$ was obtained via hydrothermal reaction of europium(III) nitrate with trimethylamine and sulfuric acid,[6] while $Dy(OH)SO_4$ was produced by reacting dysprosium(III) oxide with tetramethylammonium-hydroxide and sulfuric acid under hydrothermal conditions.[7] $Ce(OH)SO_4$ was synthesized in a slightly different manner by reacting cerium(III) nitrate with $Na_2SO_4 \cdot 10H_2O$ and NaOH under hydrothermal conditions.[8] The structural parameters of $Pr(OH)SO_4$ and $Nd(OH)SO_4$ were discussed by Fahey et al.,[9] Haschke et al.,[10] and Wickleder.[2] Besides solving the crystal structures of $La(OH)SO_4$, $Pr(OH)SO_4$, and $Nd(OH)SO_4$, Haschke et al. performed a detailed investigation of the phases that can be observed for the oxide-hydroxide-sulfate systems of these three lanthanide elements.[10] The hydrothermal synthesis and crystal structure of $Nd(OH)SO_4$ was further discussed by Zhang et al.[11] The crystal structures of $La(OH)SO_4$[12,13] and $Y(OH)SO_4$[14] were also reported. Although yttrium is not a lanthanide it can serve well for comparison purposes as it exhibits the trivalent oxidation state, and Y^{3+} has an ionic radius of 0.972 Å, which is just slightly smaller than the one of the Lu^{3+} cation at the end of the series, measuring 0.977 Å, as the smallest Ln^{3+} cation.[15] The same can be said about lanthanum as its La^{3+} ionic radius of 1.16 Å is somewhat larger than the one of cerium (1.143 Å) at the beginning of the series.

All of these compounds crystallize in the monoclinic crystal system. Although most structural parameters of the lanthanide sulfate octahydrates ($Ln_2(SO_4)_3 \cdot 8H_2O$) have been elucidated,[2,16] so far no comprehensive investigation, in regard to correlating the structural properties of an extended series of lanthanide hydroxysulfates, has been conducted. In the present work, we describe the hydrothermal preparation of a series of lanthanide hydroxysulfates, $Ln(OH)SO_4$ (Ln = Pr−Yb, except Pm), by reacting $Ln_2(SO_4)_3 \cdot 8H_2O$ with NaOH under hydrothermal conditions. We characterized these compounds via single crystal X-ray diffraction analysis, as well as FT-IR spectroscopy.

Experimental Section

General Remarks. Chemicals used as starting materials were purchased from Acros Organics, Aldrich Co., Alfa Aesar, Spectrum Chemicals, as well as Strem Chemicals and were used without further purification.

Synthesis and Characterization. Samples of $Ln_2(SO_4)_3 \cdot 8H_2O$ were weighed out and placed in Teflon linears inside Parr acid digestion vessels (Ln = Pr−Tm, except Pm). For creating the Ho analogue we utilized $Ho_2(SO_4)_3 \cdot H_2O$, and for the Yb-counterpart anhydrous $Yb_2(SO_4)_3$ was used. We employed the larger sized Parr steel autoclaves with a volume of 45 mL for all experiments (model 4744). About 0.25 g of lanthanide sulfate octahydrate (0.4−5 mmol) was weighed out for each reaction. Then ~0.75 mmol of NaOH was added and about 7 mL of deionized (DI) water was included. The vessels were sealed and

(4) Del Cul, G. D.; Nave, S. E.; Begun, G. M.; Peterson, J. R. *J. Raman Spectrosc.* **1992**, *23*(5), 267–272. Del Cul, G. D.; Nave, S. E.; Peterson, J. R. *J. Alloy. Compd.* **1993**, *193*(1−2), 194–196. Fujita, D. K.; Cunningham, B. B.; Parsons, T. C. *Inorg. Nucl. Chem. Lett.* **1969**, *5*(4), 307–313. Peterson, J. R. *Nucl. Sci. Abstr.* **1968**, *22*(4), 6292. Peterson, J. R.; Cunningham, B. B. *J. Inorg. Nucl. Chem.* **1968**, *30*(3), 823–828. Schleid, T.; Morss, L. R.; Meyer, G. *J. Less-Common. Met.* **1987**, *127*, 183–187. Templeton, D. H.; Dauben, C. H. *J. Am. Chem. Soc.* **1953**, *75*, 4560–4562.

(5) Zehnder, R. A.; Clark, D. L.; Scott, B. L.; Donohoe, R. J.; Palmer, P. D.; Runde, W. H.; Hobart, D. E. *Inorg. Chem.* **2010**, *49*, 4781–4790.

(6) Ding, S. H.; Sun, X. C.; Zhu, Y. L.; Chen, Q.; Xu, Y. *Acta Crystallogr.* **2006**, *E62*, i269–i271.

(7) Xu, Y.; Ding, S. H.; Zheng, X. *J. Solid State Chem.* **2007**, *180*, 2020–2025.

(8) Yang, Y.; Zhu, L. H.; Zeng, M. H.; Feng, X. L. *Acta Crystallogr.* **2005**, *E61*, i41–i43.

(9) Fahey, J. A.; Williams, G. J. B.; Haschke, J. M. *The Rare Earths in Modern Science and Technology*; Plenum Press: New York, 1980; Vol. *2*, pp 181−186.

(10) Haschke, J. M. *J. Solid State Chem.* **1988**, *73*, 71–79.

(11) Zhang, T.; Lu, J. *Acta Crystallogr.* **2008**, *E64*, i49.

(12) Lopez-Delgado, A.; Garcia-Martinez, O. *J. Less-Common Met.* **1989**, *149*, 109–114.

(13) Zhang, Q.; Lu, C.; Yang, W.; Chen, Q.; Yu, Y. *Inorg. Chem. Commun.* **2004**, *7*, 889–892.

(14) Wang, X.; Liu, L.; Ross, K.; Jacobson, A. J. *Solid State Sci.* **2000**, *2*(1), 109–118.

(15) Shannon, R. D. *Acta Crystallogr.* **1976**, *A32*, 751–768.

(16) Ahmed Farag, I. S.; El Kordy, M. A.; Ahmed, N. A. *Z. Kristallogr.* **1981**, *155*, 165–171. Bartl, H.; Rodek, E. *Z. Kristallogr.* **1983**, *162*, 13–15. Gebert Sherry, E. *J. Sol. State Chem.* **1976**, *19*, 271–279. Hiltunen, L.; Niinistoe, L. *Cryst. Struct. Commun.* **1976**, *5*, 561–566. Hummel, H. U.; Fischer, E.; Fischer, T.; Joerg, P.; Pezzei, G. *Z. Anorg. Allg. Chem.* **1993**, *619*, 805–810. Junk, P. C.; Kepert, C. J.; Skelton, B. W.; White, A. H. *Aust. J. Chem.* **1999**, *52*, 601–605. Podberezskaya, N. V.; Borlsov, S. *Zh. Struk. Khim.* **1976**, *17*, 186–188. Sarangarajan, R. T.; Panchanatheswaran, K.; Low, J. N.; Glidewell, C. *Acta Crystallogr.* **2004**, *E60*, i142–i144. Wei, D.; Zheng, Y. Q. *Z. Kristallogr. - New Cryst. Struct.* **2003**, *218*(3), 277–278. Wickleder, M. S. *Z. Anorg. Allg. Chem.* **1999**, *625*, 1548–1555.

placed in a conventional laboratory oven at 170 °C for 10 days. At the end of the heating period the vessels were taken out of the oven and allowed to cool down to ambient temperature on the lab bench. Once at room temperature the Parr vessels were opened. Solid materials were obtained, which were submerged in the mother liquor. The resulting materials were transferred into 20 mL scintillation vials. Larger chunks of material were crushed into smaller pieces using a spatula. The vial was then filled with DI water, closed, and shaken to wash the products and remove any soluble starting materials or byproducts. The products were allowed to settle down at the bottom of the vial, and the water was decanted and discarded. This rinsing process was repeated three more times. The remaining products were composed of a mixture of crystalline materials that contained single crystals of X-ray quality as well as microcrystalline and/or amorphous powders. Small amounts of products were stored in scintillation vials with small quantities of DI water until a single crystal was chosen for X-ray structural analysis. Small samples of the remaining materials were dried in a laboratory oven at 110 °C. The dry samples were homogenized using a mortar and pestle and then characterized via FT-IR spectroscopy.

IR spectra were collected on a PerkinElmer Spectrum 100 FT-IR Spectrometer using KBr pellets. Spectral resolution was typically 4 cm^{-1}, and average data sets included 64 scans.

X-ray Structure Determination. Crystals of the $Ln(OH)SO_4$, with Ln = Sm, Gd, Tb, Ho, Tm, and Yb, were mounted on a Mitegen 20 μm micromesh mount using a small amount of mineral oil. The data were collected on a Bruker Smart APEX charge-coupled-device (CCD) diffractometer with an ApexII software upgrade, and a KRYO-FLEX liquid nitrogen vapor cooling device. Data were collected at 100 K. The instrument is equipped with a graphite monochromatized MoKα X-ray source (λ = 0.71073 Å) with MonoCap X-ray source optics. Hemispheres or spheres of data were collected using ω scans. Data collection and initial indexing and cell refinement were handled using APEX II software.[17] Frame integration and final cell parameter calculations were carried out using the SAINT+ software as implemented in Apex II. The data were corrected for absorption using the SADABS program. The structures were solved either by direct methods, Patterson methods, or by isomorphous replacement, based on known structures and were refined by full matrix least-squares against F^2 with all reflections using the SHELXTL V6.14 package.[18,19] Non hydrogen atoms were refined anisotropically. All H atoms (OH groups) were treated based on the data quality (refined with appropriate restraints where possible, placed in calculated positions where not). Additional details of hydrogen atom treatment and software versions may be found in the Supporting Information cif file.

Intensity data for crystals of $Ln(OH)SO_4$, with Ln = Pr, Nd, Eu, Dy, and Er were collected at 90 K on a Nonius KappaCCD diffractometer equipped with an Oxford Cryosystems Cryostream sample cooler and a graphite monochromated MoKα X-ray source (λ = 0.71073 Å). Data were collected using ϕ and ω scans to $2\theta > 80°$ and corrected for absorption using the multiscan method using DENZO and SCALEPACK.[20] Structures were solved by direct methods using SIR[21] and refined on F^2 using SHELXL.[19] Hydrogen atoms were visible in difference maps, but were placed in idealized positions with O−H distance 1.00 Å, except for the Dy structure, for which the H position was refined.

Results and Discussion

Synthesis. The treatment of the various $Ln_2(SO_4)_3 \cdot 8H_2O$ compounds with NaOH under hydrothermal conditions at 170 °C for 10 days resulted in the formation of water insoluble products that formed either millimeter-sized crystals, microcrystalline powders, amorphous solids, or a mixture of these. The crystal forms ranged from loose, thin, long individual needles to elaborate three-dimensional (3D) sprays, platelets, or rectangular blocks. The formation of the anhydrous $Ln(OH)SO_4$ compounds seems to require the presence of sodium hydroxide as opposed to the $Ln(OH)_2Cl$ compounds whose formation seems to proceed via hydrolyzation of the Ln^{3+} cations in the remaining waters of crystallization after partial dehydration.[5,22] With large amounts of water present in the reaction mixtures for this series of lanthanide hydroxysulfates, a thermal dehydration process appears unlikely. Experiments performed without the addition of NaOH did not produce any crystalline materials in X-ray quality, and mostly starting material was unaltered after the reaction period. We attribute the ready formation of the anhydrous lanthanide hydroxysulfates to be governed thermodynamically, since a significant entropy increase can be expected because the formation of the resulting coordination polymer is accompanied by the liberation of a larger number of small entities (reaction 1), comparable to reactions involving a chelating effect.[23]

$$n\mathrm{Ln_2(SO_4)_3 \cdot 8H_2O} + 2n\mathrm{NaOH} \rightarrow 2(\mathrm{Ln(OH)SO_4})_n + n\mathrm{Na_2SO_4} + 8n\mathrm{H_2O} \quad (1)$$

Solid State Structures. All lanthanide hydroxysulfates crystallize in the monoclinic crystal system (space group $P2_1/n$). Our structural data at low temperatures (90 and 100 K) are in good agreement with the previously reported structures for $Pr(OH)SO_4$,[2,9,10] $Nd(OH)SO_4$,[10,11] $Eu(OH)SO_4$,[6] and $Dy(OH)SO_4$.[7] To our knowledge the single crystal structures of $Sm(OH)SO_4$, $Gd(OH)SO_4$, $Tb(OH)SO_4$, $Ho(OH)SO_4$, $Er(OH)SO_4$, $Tm(OH)SO_4$, and $Yb(OH)SO_4$ have not been solved previously and are reported here for the first time. Numerous trials synthesizing $Ce(OH)SO_4$ by us resulted in the formation of $NaCe(SO_4)_2 \cdot H_2O$. The structure of this compound has been discussed numerous times.[24] This compound was reported to crystallize in the trigonal crystal system with space group $P3_221$ or $P3_121$ with the water oxygen atom showing a degree of disorder. These structures were determined at room temperature, while our initial data were collected at 100 K, at which temperature the crystals were found to be merohedrally twinned with the space group $P3_2$. The phase transition between the low temperature structure and the one at room temperature will be discussed elsewhere. We were unsuccessful in obtaining single crystals of $Lu(OH)SO_4$. We did not perform any powder XRDs on the bulk samples, thus, we cannot

(17) *Apex2 v2009.7−0* (*includes SAINT V7.66A and SADABS 2008/1*); Bruker AXS Inc: Madison, WI, 2009.
(18) *SHELXTL 6.14*; Bruker AXS Inc: Madison, WI, 2003.
(19) Sheldrick, G. M. *Acta Crystallogr.* **2008**, *A64*(1), 112–122.
(20) Otwinowski, Z.; Minor, W. *Macromolecular Crystallography, part A.*; Academic Press: New York, 1997; Vol. *276*.
(21) Altomare, A.; Burla, M. C.; Camalli, M.; Cascarano, G. L.; Giacovazzo, C.; Guagliardi, A.; Moliterni, A. G. G.; Polidori, G.; Spagna, R. *J. Appl. Crystallogr.* **1999**, *32*, 115–119.
(22) Buzagh-Gere, E.; Gal, S.; Simon, J. *Inst. Gen. Anal. Chem.* **1974**, *28*, 25–30. Kipouros, G. J.; Sharma, R. A. *J. Less-Comm. Met.* **1990**, *160*(1), 85–99. Matthes, F.; Haessler, G. *Z. Chem.* **1963**, *3*(2), 72–73. Petzold, D.; Naumann, R. *Freib. Forsch. A* **1979**, *A616*, 75–86. Petzold, D.; Naumann, R. *J. Therm. Anal.* **1980**, *19*(1), 25–34.
(23) Schwarzenbach, G. *Helv. Chim. Acta* **2004**, *35*(7), 2344–2359.
(24) Blackburn, A. C.; Gerkin, R. E. *Acta Crystallogr.* **1995**, *C51*, 2215–2218. Lindgren, O. *Acta Chem. Scand.* **1977**, *31*, 591–594.

Table 1. Crystal Data and Summary of Data Collection and Refinement for $Ln(OH)SO_4$, Ln = Pr−Yb (except Pm)

Formula	Pr(OH)-SO_4	Nd(OH)-SO_4	Sm(OH)-SO_4	Eu(OH)-SO_4	Gd(OH)-SO_4	Tb(OH)-SO_4	Dy(OH)-SO_4	Ho(OH)-SO_4	Er(OH)-SO_4	Tm(OH)-SO_4	Yb(OH)-SO_4
fw	253.98	257.31	263.42	265.03	270.33	271.99	275.57	278.01	280.33	282.00	286.11
a (Å)	4.4933(8)	4.4733(10)	4.4350(12)	4.4238(10)	4.3993(10)	8.008(2)	7.9819(15)	7.9465(12)	7.9548(12)	7.9064(18)	7.871(3)
b (Å)	12.4922(15)	12.432(2)	12.301(3)	12.279(3)	12.219(3)	10.894(3)	10.924(2)	10.8807(16)	10.8906(15)	10.810(2)	10.836(4)
c (Å)	6.8613(10)	6.8346(12)	6.7780(19)	6.7609(15)	6.7302(14)	8.186(3)	8.1508(10)	8.0925(12)	8.0880(12)	8.0439(18)	8.017(3)
β (deg)	106.335(7)	106.396(9)	106.456(3)	106.477(11)	106.456(2)	93.634(4)	93.617(7)	93.7141(19)	93.874(9)	93.838(3)	93.986(5)
V (Å^3)	369.59(10)	364.63(12)	354.62(17)	352.17(14)	346.95(13)	712.7(4)	709.3(2)	698.24(18)	699.08(18)	685.9(3)	682.2(4)
space group	$P2_1/n$	$P2_1/n$	$P2_1/n$	$P2_1/n$	$P2_1/n$	$P2_1/n$	$P2_1/n$	$P2_1/n$	$P2_1/n$	$P2_1/n$	$P2_1/n$
Z	4	4	4	4	4	8	8	8	8	8	8
D_c (Mg m^{-3})	4.564	4.687	4.934	4.999	5.175	5.069	5.161	5.289	5.327	5.461	5.571
μ (mm^{-1})	13.632	14.695	17.027	18.28	19.593	20.310	21.54	23.138	24.484	26.352	27.903
$F(000)$	464	468	476	480	484	976	984	992	1000	1008	1016
T (K)	90.0(5)	90.0(5)	100(2)	90.0(5)	100(2)	100(2)	90.0(5)	100(2)	90.0(5)	100(2)	100(2)
refln. indep.	2393	2337	1081	2192	2209	2170	4447	2070	4382	2111	2138
refln. $I > 2\sigma(I)$.	2211	2121	1006	2065	1072	1860	4009	1895	3248	1830	1798
R_{int}	0.022	0.030	0.0277	0.038	0.0246	0.0564	0.027	0.0235	0.051	0.0374	0.0609
R1($I > 2\sigma$)	0.027	0.037	0.0106	0.038	0.0182	0.0286	0.030	0.0248	0.043	0.0231	0.0262
wR2($I > 2\sigma$)	0.067	0.095	0.0449	0.107	0.0399	0.0643	0.069	0.058	0.088	0.0498	0.0556

exclude that we obtained phase mixtures of these compounds. The IR-spectra, especially the positions and number of OH vibrations, suggest however, that we obtained fairly pure phases of these materials. For better comparison of metrical parameters we reinvestigated the previously described complexes and determined the X-ray single crystal structures of the whole extended series at 90 or 100 K. In Table 1 we provide the crystallographic parameters for all structures.

For this series of lanthanide hydroxysulfates we found that all $Ln(OH)SO_4$ complexes arrange in extended 3D lattice structures. Although all $Ln(OH)SO_4$ compounds crystallize monoclinic with space group $P2_1/n$, they are not isostructural throughout the entire series. The lighter $Ln(OH)SO_4$ complexes from Pr−Gd (except Pm) are isostructural and exhibit identical $Ln(OH)SO_4$ units, in which each lanthanide metal center is coordinated to 9 surrounding oxygen atoms. They hardly show any changes with regard to their unit cell parameters including the angle "β". Between Gd and Tb we discovered a "break" in the crystal structure, accompanied by doubling of the unit cell volume and a reduction of the coordination number from 9 to 8 where it remains for the heavier analogues between Tb and Yb. These heavier $Ln(OH)SO_4$ complexes are again isostructural and exhibit two crystallographically independent $Ln(OH)SO_4$ units. These 8 coordinate complexes do not undergo significant changes in regard to their unit cell parameters either. Ln−O bond distances for this series lie between 2.20 and 2.80 Å and do not exceed 2.87 Å, which was reported to be the longest Ln−O bond distance in 9-coordinate $La(OH)SO_4$.[13] For clarity we will discuss the structural properties of the lighter $Ln(OH)SO_4$ complexes first and then address their heavier analogues as their structural behavior is somewhat more complex.

Representative of all lighter $Ln(OH)SO_4$ complexes we illustrate the structural properties for $Gd(OH)SO_4$. Each metal center is coordinated to 6 O-atoms stemming from sulfate tetrahedrons and 3 OH groups. Each hydroxy group is bound μ^3 to three Ln atoms and each sulfate unit incorporates two oxygen atoms that bind μ^2 to two Ln^{3+} ions. The other two sulfate oxygen atoms coordinate with one bond to one Ln central atom, respectively. Figure 1 illustrates the resulting highly linked network of hydroxy groups, sulfate entities, and Ln-metal centers in the "bc" plane. Via the bridging hydroxy groups the Ln-central atoms form infinite Ln-O-Ln-O-Ln zigzag chains along the "a" axis. Four of these chains run through one unit cell, so that each unit cell accommodates four complete formulas of $Ln(OH)SO_4$. Figure 1a) demonstrates how the third bond of each OH unit connects to the next Ln-central atom in the direction of the "bc" diagonal.

In the direction "c" of the same layer two oxygen atoms of the sulfate tetrahedra link in a μ^2 fashion to three different Ln-metal centers. The other two sulfate oxygen atoms coordinate to one Ln-central atom respectively, of which one belongs to the adjacent layer (direction "b"). Figure 1b) emphasizes the 3D nature of such lattices. These compounds form layered structures, in which layers of LnO_9-polyhedra are confined to the "ac" plane and they are connected via face and edge −sharing, resulting in infinite chains elongating along the "a" and "c" axes. The individual "ac" layers are tied together by the sulfate entities along the "b" axis. Moreover, the hydroxy groups exhibit two different hydrogen bonds, which are connecting to the adjacent layers. The LnO_9-coordination-polyhedra could be described as distorted tricapped trigonal prisms, as it is typical for the UCl_3 type structure,[25] or as distorted monocapped square antiprisms.

The latter description seems to fit these structural motifs slightly better, therefore, the lighter $Ln(OH)SO_4$ complexes are rather related to the PbClF type structure.[26] An illustration of the LnO_9 polyhedron can be viewed in Supporting Information, Figure S1a. Figure 2a depicts how two of the monocapped square antiprisms are combined via face sharing through their squared bases forming Ln_2O_{14}-coordination-polyhedra. These Ln_2O_{14}-polyhedra connect via edge sharing, resulting in infinite chains expanding along the "c" axis. The oxygen atoms utilized in the edge sharing of these polyhedra stem from sulfate units. Figure 2b showcases how individual chains are linked in the "a" direction via edge sharing, resulting in the above-mentioned Ln−OH−Ln zigzag formations.

(25) Taylor, J. C. W.; P., W. *Acta Crystallogr., Sect. B: Struct. Sci.* **1974**, *B30*(12), 2803–2805.

(26) Hassan, E. H.; Akbarzadeh, F.; Hashemifar, H.; Mokhtari, A. *J. Phys. Chem. Solids* **2004**, *65*(11), 1871–1878. Meyer, G.; Schleid, T. *Z. Anorg. Allg. Chem.* **1986**, *533*, 181–185. Shen, Y. R.; Englisch, U.; Chudinovskikh, L.; Porsch, F.; Haberkorn, R.; Beck, H. P.; Holzapfel, W. B. *J. Phys.: Condens. Matter* **1994**, *6*, 3197–3206.

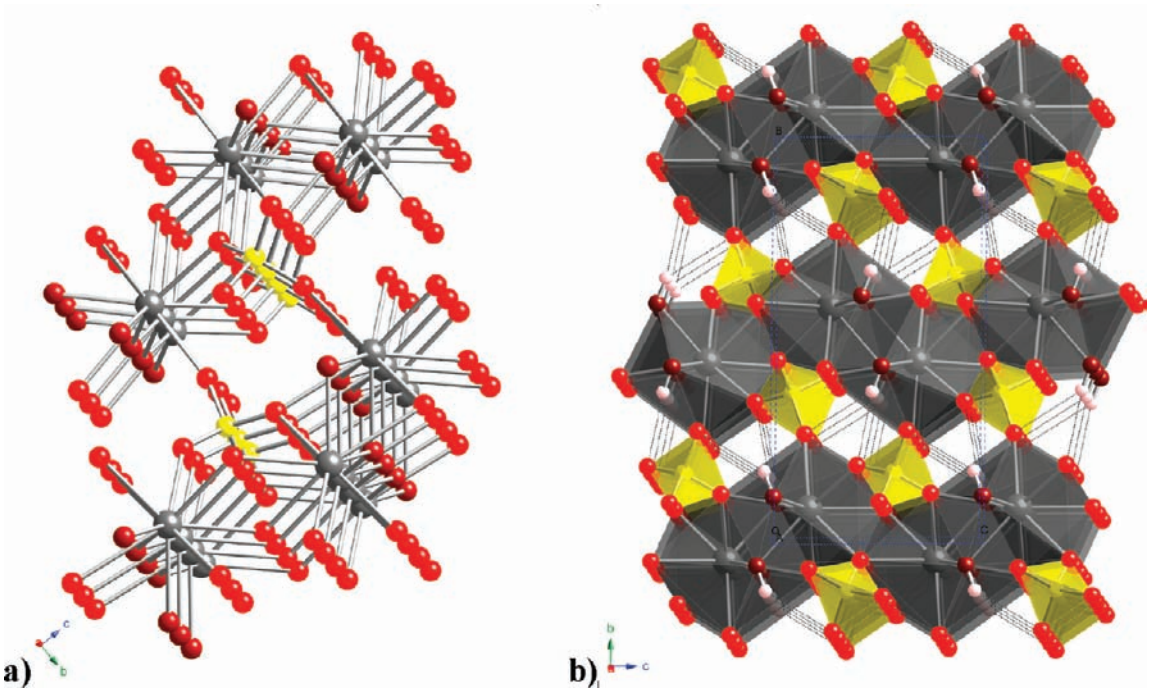

Figure 1. Highly linked network of hydroxy groups, sulfate units, and the metal centers in the "*bc*" plane of monoclinic $Gd(OH)SO_4$ (gray = Gd, yellow = S, red = O (from SO_4^{2-} units), maroon = O (from OH^- units), white = H). (a) Each hydroxy group is coordinated to three metal centers. The metal centers form zigzag chains with the hydroxy groups in the "*a*" direction, while the third bond of each hydroxide group connects to the next metal center along the "*bc*" diagonal (hydrogen atoms are omitted for clarity). (b) Top view along "*a*" direction, illustrating the role of the sulfate tetrahedrons in tying together the layers of this structure in the "*b*" direction. One can also recognize the OH groups engaging in two hydrogen-bonds toward sulfate O atoms of adjacent layers.

The heavier $Ln(OH)SO_4$ complexes (Ln = Tb−Yb) display a significantly different structural pattern. Since they are also isostructural among each other, we will present the structural details of $Tb(OH)SO_4$ as representative of all heavier lanthanide hydroxysulfates. What becomes apparent is that the resulting 3D networks of the heavier lanthanide hydroxysulfates incorporate one-dimensional (1D), infinite channels of Ln-metal centers that are connected by Ln-O-Ln zigzag chains along the "*c*" axis. These zigzag chains stem from the hydroxy groups, as observed for the lighter Ln-analogues. Figure 3 illustrates that two of these channels are grouped together, exclusively by hydroxy groups parallel to the "*a*" axis, forming a double zigzag chain, and that they can be viewed as "islands" within the "*ab*" plane that are surrounded and linked together in "*a*" and "*b*" directions by six sulfate tetrahedra. The most striking difference compared to the lighter series is that the heavier $Ln(OH)SO_4$ counterparts exhibit two crystallographically different units. The view on top of the "*ab*" plane allows one to recognize that these different units are slightly twisted toward each other, while elongating along the "*c*" axis in an alternating manner. Moreover, each Ln-oxygen coordination polyhedron is linked to one crystallographically identical polyhedron, and to one crystallographically alternated polyhedron via edge sharing. Each polyhedron is further connected to a second crystallographically alternated polyhedron through face sharing and to a third crystallographically alternated polyhedron via corner sharing in each group of 1D channels, as can be seen in Figure 4. In Figure 3a we point out the crystallographically different Tb atoms by a darker gray color and the different S atoms by a darker yellow color. Although there are two crystallographically independent sulfate and hydroxide oxygen types we did not alter their color for simplicity. One can clearly recognize the Ln-O-Ln double zigzag chains linking the lanthanide metal centers along the "*c*" axis. As observed for the lighter lanthanide sulfates, each hydroxy group is coordinated μ^3 to three Ln-metal centers. The sulfate tetrahedra only incorporate one oxygen atom that links two crystallographically different Ln-central atoms in a μ^2 manner respectively within the "*c*" direction.

The other three sulfate oxygen atoms coordinate with only one bond to one Ln central atom respectively. Each of the two crystallographically independent hydroxy groups exhibits one hydrogen bond respectively, bridging two "islands" along the "*ab*" diagonal. The structural motifs of the heavier complexes from Tb−Yb are composed of 8-coordinate polyhedra that could be best depicted as distorted square antiprisms. An illustration of two crystallographically different LnO_8 polyhedra linked together via hydroxy groups in an edge sharing fashion, parallel to the "*a*" axis and resulting in an Ln_2O_{14} polyhedron, can be viewed in Supporting Information, Figure S1b. In Figure 4 we demonstrate how 1D channels of Ln-metal−oxygen polyhedra stretch infinitely along the "*c*" axis. Four LnO_8 polyhedra assemble to Ln_4O_{22} units via edge and face sharing involving two units of crystallographically different Ln_2O_{14} entities. These Ln_2O_{14} segments connect via face sharing with each other, resulting in 1D "islands".

The S−O bond distances of the sulfate units across the entire series range between 1.452(3) and 1.504(3)Å, which agrees with the structural properties commonly observed for sulfates in various compounds.[27] The individual S−O distances vary within 0.01 and 0.017 Å, which is insignificant

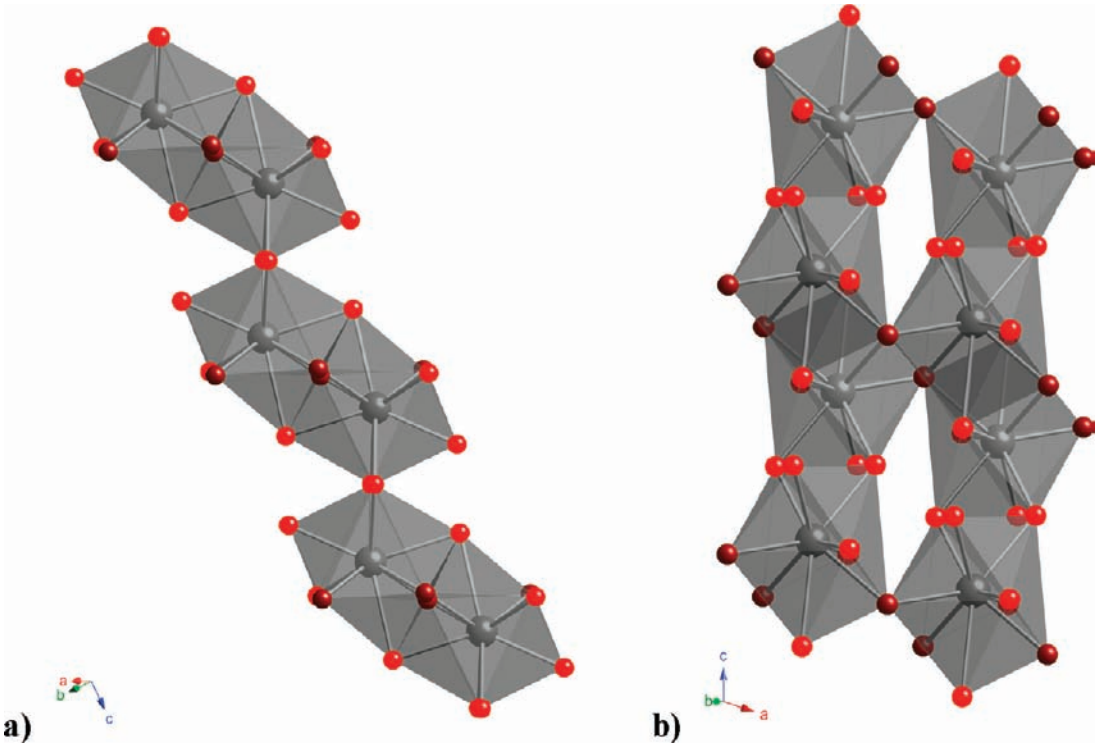

Figure 2. Arrangement of LnO_9-coordination polyhedra, whose structural motif can most closely be portrayed as a distorted form of a monocapped square antiprism (gray = Gd, yellow = S, red = O (from SO_4^{2-} units), maroon = O (from OH^- units), hydrogen atoms are omitted for clarity). Two monocapped square antiprisms share their squared base resulting in Ln_2O_{14}-polyhedra. (a) Infinite chain of Ln_2O_{14}-polyhedra connecting via edge sharing along the "*c*" axis of monoclinic $Gd(OH)SO_4$. (b) Infinite expansion of Ln_2O_{14}-polyhedra chains in the "*a*" direction via edge sharing, utilizing hydroxy groups that are involved in the Ln−OH−Ln zigzag formation (only two connected chains shown here).

as compared to the reduction of Ln−O bond distances along the series. Thus, the sulfate units do not suffer any noticeable changes in bond distances along the series of lanthanide hydroxysulfates (including the two crystallographically different SO_4^{2-} entities for the heavier Ln-elements). Furthermore, their O−S−O angles lie within the expected range of the tetrahedron angle with a variance of ±3°. Consequently, the SO_4^{2-} units can be viewed as hard rigid tetrahedra that hardly vary in shape and size.

After pointing out the general structural properties of the lanthanide hydroxysulfates we would like to focus on the structural trends within this series and compare them with other series such as the hydrated lanthanide sulfates and the lanthanide bis-hydroxychlorides. Between Gd and Tb the topology changes to the other structural arrangement, which shows completely different values for the three unit cell axes and the β angle. Figure 5a shows cell parameters of these two $Ln(OH)SO_4$ complexes, and the gradual changes of the *a*, *b*, and *c* axis values within each of the two isostructural series. Both series show a similar trend with a slight gradual decrease in length for all the axes, with the largest change observed (both, in total as well as in percent of the axis length) for the *b* axis of the lighter lanthanide complexes.

The individual Ln−O distances follow the trend of the unit cell axes and slightly decrease from Pr to Gd. After a noticeable readjustment as a result of the change in the crystal lattice this trend is continued between Tb and Yb. A scheme illustrating the trends of the Ln−O bond lengths can be found as Supporting Information, Figure S3.

We attribute the trends observed for this series to the high rigidity of the crystal lattice, combined with the decreasing ionic radius of the lanthanides. The rigidity seems to be a direct result of the 3D linkage of lanthanide metal centers by sulfate tetrahedra. Considering the bridging function of the sulfate entities between the "*ac*" layers in "*b*" direction for these lighter analogues, the reduction of the ionic radius should be without noticeable consequences for the crystal lattice in this dimension. Figure 1 implies that the lessening of the ionic radius is rather likely to impose an effect on the crystal lattice in respect with direction "*c*". Three Ln-metal centers are linked by one sulfate unit via three oxygen atoms involving five Ln-O coordinations. Figure 6a illustrates that the crystal lattice is experiencing increasing strain with decreasing ionic radius because of the rigidity of the sulfate tetrahedra. With the Ln−O bond distances shortening along the series and the sulfate entities' inability to adjust sufficiently in size or geometry the energy level for this structural arrangement seems to increase steadily until it becomes unfavorable for the $Ln(OH)SO_4$ counterparts beyond Gd. Consequently, the heavier counterparts starting with Tb offer an alternative structure type, which we believe, is energetically more favorable, as it allows adequate space for the further closing in of the Ln-metal centers in a less crowded manner. For the lighter Ln-$(OH)SO_4$ the bond angles between the five Ln-metal centers, oxygen atoms, and the S atom of the sulfate unit within the "*ac*" layer respond to the declining space

(27) Cole, W. F.; Lancucki, C. J. *Acta Crystallogr.* **1974**, *30*(4), 921–929. Zalkin, A.; Ruben, H.; Templeton, D. H. *Acta Crystallogr.* **1962**, *15*, 1219–1224.

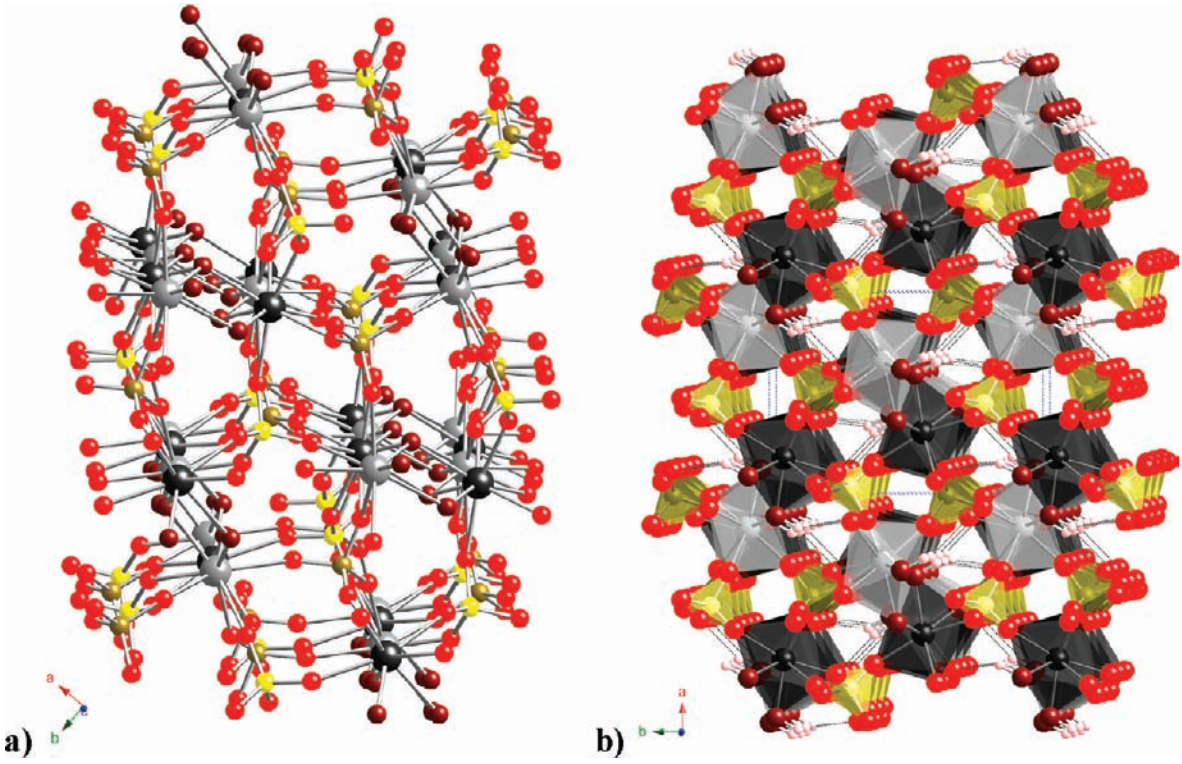

Figure 3. Highly linked network of hydroxy groups, sulfate units, and the metal centers in the "*ab*" plane of monoclinic $Tb(OH)SO_4$ (gray = Tb1, dark gray = Tb2, yellow = S1, dark yellow = S2, red = O1−O8 (from SO_4^{2-} units), maroon = O9 and O10 (from OH^- units), white = H). (a) Each hydroxy group is coordinated to three metal centers. The metal centers form zigzag chains with the hydroxy groups within the "*c*" direction, while the third bond of each hydroxide group is connecting to the next metal center parallel to the "*a*" axis (hydrogen atoms are omitted, and sizes of S as well as O atoms are reduced in respect to the Ln ions for clarity). (b) Top view along the "*c*" direction, illustrating the role of the sulfate tetrahedrons in tying together the 1D channels ("islands") of Ln-coordination polyhedra of this structure in the "*a*" as well as the "*b*" direction. One can also recognize the OH groups engaging in two hydrogen-bonds bridging two layers along the "*ab*" diagonal.

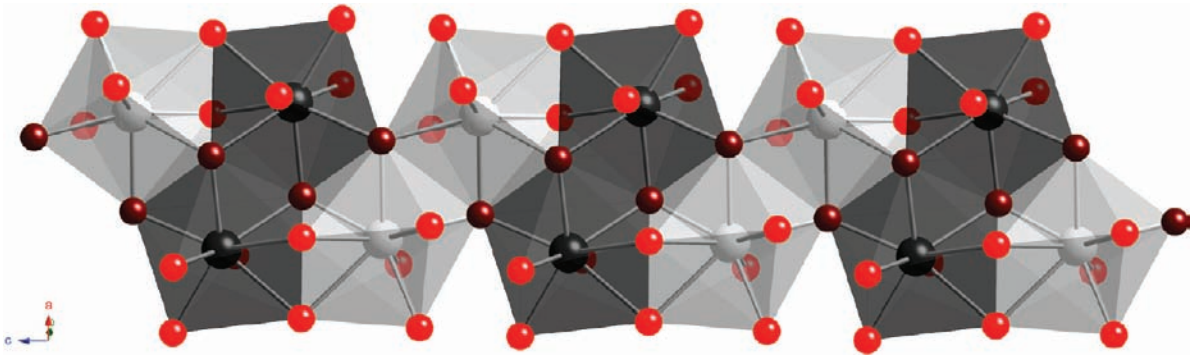

Figure 4. Infinite channels of two crystallographically different TbO_8 polyhedra extending along the "*c*" axis (gray = Tb1, dark gray = Tb2, maroon = O9 and O10 (from OH- units), red = O1−O8 (from crystallographically different SO_4^{2-} units), hydrogen atoms are omitted, and sizes of O atoms are reduced in respect to the Ln ions for clarity). Two crystallographically different LnO_8 polyhedra connect via face sharing in the "*c*" direction, resulting in Ln_2O_{14} motifs, which are tied together by hydroxy groups in an edge sharing fashion, parallel to the "*a*" axis. This causes the formation of Ln_4O_{22} assemblies that extend along the "*c*" axis via edge sharing.

availability between the coordination polyhedra via slight adjustments. The trends of these five bond angles correlated to the decreasing ionic radius are listed in Table 2 and visualized in Figure 6b. With Figure 6a it becomes apparent that each SO_4^{2-} tetrahedron experiences an increasing degree of torsion into the "*ac*" plane in anticlockwise manner. While the Ln−O bond distances shorten along the series of lighter $Ln(OH)SO_4$ complexes, the enhanced degree of tension causes the Ln−O−S bond angles 1 and 2 to expand, while narrowing angles 3 and 5. This process enhances the torque on the sulfate unit resulting in an anticlockwise partial spin of the sulfate tetrahedron into the "*ac*" layer.

Apparently the tension buildup within the coordination sphere of the $Ln(OH)SO_4$ complexes raises the energy level, which becomes more awkward for the heavier counterparts beyond Gd. This increased strain is alleviated by a complete rearrangement of the crystal structure going along with the reduction of the coordination number from 9 to 8, which seems to lower the energy level, so that this arrangement becomes the preferred structure type for the heavier analogues. The different

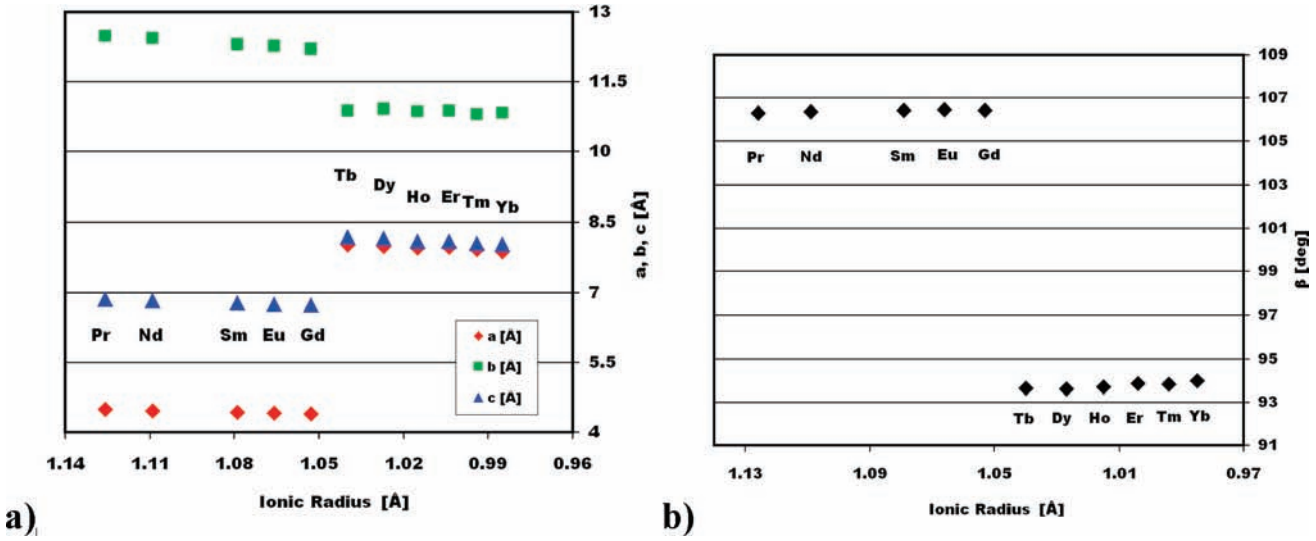

Figure 5. (a) Cell parameters *a*, *b*, and *c* (Å) of $Ln(OH)SO_4$ and (b) cell parameter β (deg) of $Ln(OH)SO_4$ in correlation with trivalent lanthanide(III) ionic radius (Å).[15].

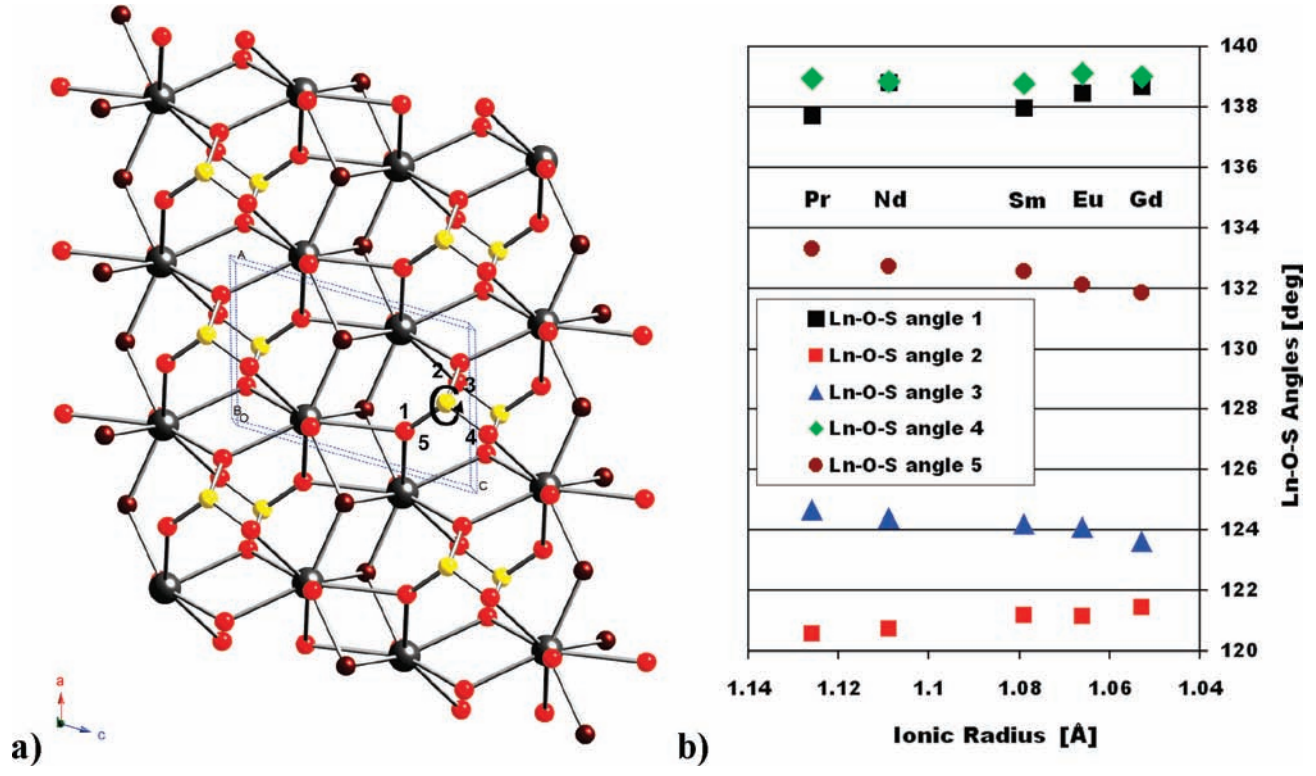

Figure 6. (a) View onto the "*ac*" layer of $Gd(OH)SO_4$ illustrating how the reduction of the ionic radius along with the shortening of the Ln−O bond lengths causes an increase of strain onto the crystal lattice because of the rigidity of the sulfate units (gray = Gd, yellow = S, red = O (from SO_4^{2-} units), maroon = O (from OH^- units), hydrogen atoms and the sulfate oxygen atoms bridging to the next layer in "*b*" direction are omitted for simplicity). The lattice seems to counteract the tension buildup by adjusting the torsion of the sulfate tetrahedra. The bond angles, that are composed of the surrounding five Ln- and oxygen atoms (the sixth Ln- and O atoms, residing in the adjacent "*ac*" layer, are omitted) as well as the sulfur atom are labeled clockwise with numbers 1−5. (b) Trends of these 5 depicted bond angles for the lighter $Ln(OH)SO_4$ complexes with Ln = Pr−Gd, in correlation with trivalent lanthanide(III) ionic radius (Å).[15] With Ln−O−S angles 1 and 2 slightly increasing, while angles 3 and 5 experience a small decline, the sulfate entity exhibits an increasing degree of torsion in anticlockwise fashion between Pr and Gd.

arrangement of the lattice structure between Tb and Yb, resulting in the linkage of the grouped chains of LnO_8 polyhedra in "*a*" and "*b*" directions via SO_4^{2-} tetrahedra, including the introduction of two crystallographically independent $Ln(OH)SO_4$ units, seems to enhance the flexibility of the lattice.

For clockwise labeling of the five angles around the sulfate entity, please see Figure 6a.

Throughout the series of heavier $Ln(OH)SO_4$ complexes, one would expect that tension on the crystal lattice would mainly build up within the "*c*" direction because of one sulfate oxygen atom coordinating to two adjacent

Table 2. Bond Angles for Five of the Six Ln−O−S Bonds Surrounding One SO_4^{2-} Tetrahedron in One "*ac*" Layer (Ln = Pr−Gd)

β and Ln−O−S bond angles	**1** [deg]	**2** [deg]	**3** [deg]	**4** [deg]	**5** [deg]
$Pr(OH)SO_4$	137.725	120.575	124.669	138.947	133.309
$Nd(OH)SO_4$	138.801	120.74	124.398	138.832	132.737
$Sm(OH)SO_4$	137.977	121.203	124.195	138.778	132.556
$Eu(OH)SO_4$	138.472	121.158	124.118	139.117	132.117
$Gd(OH)SO_4$	138.674	121.450	123.637	139.03	131.867

Ln-metal centers. The increasing strain along these heavier Ln-elements seems to be counteracted by the somewhat twisted arrangement of the crystallographic different LnO_8 polyhedra and SO_4^{2-} tetrahedra along the "*c*" axis.

As far as our investigation of these complexes goes, we can only provide data up to the Yb-complex. However, since yttrium hydroxysulfate has been reported to exhibit the same type of crystal lattice along with 8-coordinate metal centers,[14] based on the Y^{3+} ionic radius,[15] we can comfortably predict that the structural properties of Lu hydroxysulfate will match the observed trends well.

These trends complement the knowledge well that we gained from our previous investigation of a series of lanthanide bis-hydroxychlorides. The $Ln(OH)_2Cl$ complexes that we discussed in our recent manuscript form a 3D crystal lattice that is tied together only by hydrogen bonding in the "*c*" direction. For a series of anhydrous lanthanide inorganic ligand complexes it is not surprising that the $Ln(OH)_2Cl$ complexes exhibit a fairly rigid crystal lattice that is placed under increasing amounts of strain as the ionic radius, and thereby, the Ln-ligand bond distances decrease. Since the $Ln(OH)_2Cl$ series does not incorporate any larger rigid entities, such as sulfate, carbonate, or phosphate ligands, the crystal lattice alleviates the rising tensions along the series via various sophisticated adjustments in regard to the unit cell parameters *b* and β. Parameters *a* and *c* show a gradual decrease with increasing atomic number, at the same time *b* shows intense fluctuations. While absorbing the increasing strain through these adjustments in the "*b*" direction, the crystal lattice of the $Ln(OH)_2Cl$ complexes maintains the structural motif of the Ln-ligand polyhedra with a coordination number of 8 throughout the entire series.[5] In contrast, the lanthanide hydroxysulfates deal with an elevated level of rigidity and therefore, seem to experience an energy increase to awkward levels. We believe that the energetic properties of the crystal system are improved via the described rearrangement of the crystal lattice. This change in the crystal structure takes place between the Gd and Tb complexes, while going along with the reduction of the structural motif from a 9-coordinate distorted monocapped square antiprism to an 8-coordinate distorted square antiprism. The behavior of the crystal lattice along this series is well represented by the trend of the unit cell volume correlated to the ionic radius as depicted in Figure 7.

Between Pr and Gd a gradual decrease of the unit cell volume takes place. At this point the crystal lattice rearranges and this is reflected by the fact that the unit cell volume for the following Tb-analogue is increased to the level of the samarium complex (after dividing by the number of crystallographically distinct formula units to account for the two distinct entities in the structures of the heavier lanthanides). Apparently, because of the change

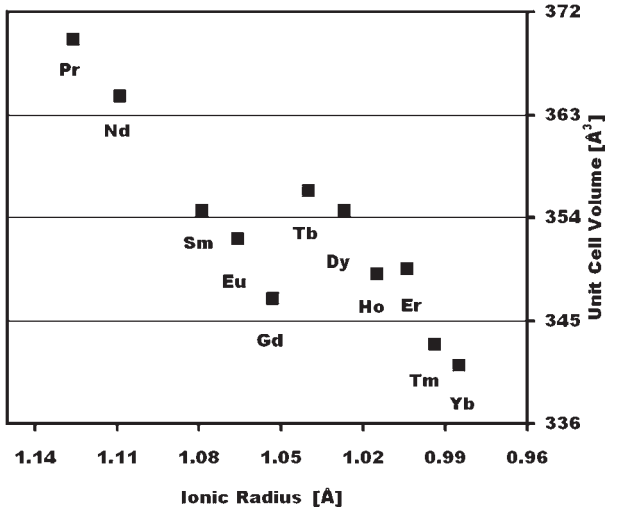

Figure 7. Unit cell volume per four formula units in correlation with trivalent lanthanide(III) ionic radius (Å).[15]

of coordination sphere and the structural motif of the coordination polyhedra, the scaled unit cell volume gains an adequate amount of space that supposedly lowers the energy profile of the system, while accommodating the ligands around the smaller Ln-metal centers between Tb and Yb. In fact, one can observe a further gradual decline of the unit cell volume for the complexes beyond Tb (Figure 7). The Tm complex is the first counterpart whose unit cell volume is smaller than observed for the Gd-$(OH)SO_4$. In comparison, the unit cell volume of the $Ln(OH)_2Cl$ complexes becomes gradually smaller with decreasing ionic radius at first. Between Tb and Ho the volume does not change, while for Er the volume is somewhat increased, to decline in a gradual manner between Er and Yb. The cell volume of the Lu-analogue is slightly larger again than the one of $Yb(OH)_2Cl$. A scheme illustrating this trend is placed in the Supporting Information, Figure S4. Apparently the fluctuations for the cell parameter *b* are sufficient to provide enough space for the coordination polyhedra along the series of lanthanide bis-hydroxychlorides as the cell volume does not decline below 137.25 $Å^3$.[5]

In essence, the structural behavior within series of inorganic, anhydrous lanthanide mixed ligand complexes are rather complicated as the resulting crystal lattices are more or less rigid. The structural trends in series of hydrated, inorganic lanthanide compounds are rather straightforward. For instance, the series of lanthanide sulfate octahydrate complexes ($Ln_2(SO_4)_3 \cdot 8H_2O$), which we employed as starting materials, show some very simple structural trends.[2,16] These compounds form two-dimensional (2D) open frameworks that are connected within the third dimension via hydrogen bonding stemming from the water molecules that coordinate to the metal centers. We correlated the various unit cell parameters from diverse publications[2,16] with the decreasing ionic radius of the lanthanide elements. The unit cell parameters *a*, *b*, and *c* show a general trend of a very small increase along the series, while the unit cell angle, on average, stays fairly constant. We provide schemes for these correlations in the Supporting Information, Figure S5. The sulfate units link the Ln-metal centers in a very straightforward fashion in two dimensions.

Table 3. Infrared Vibrational Frequencies for Monoclinic $Ln(OH)SO_4$ Compounds [cm^{-1}]

complex	ν OH_I	ν OH_{II}	δ $OH_{I,II}$	δ $OH_{I',II'}$	δ OH_{II}
$Pr(OH)SO_4$	3486		738	837	
$Nd(OH)SO_4$	3486		745	845	
$Sm(OH)SO_4$	3486		756	855	
$Eu(OH)SO_4$	3488		759	860	
$Gd(OH)SO_4$	3493		765	866	
$Tb(OH)SO_4$	3495	3553	744	859	720
$Dy(OH)SO_4$	3496	3550	755	862	755
$Ho(OH)SO_4$	3499	3559	759	867	730
$Er(OH)SO_4$	3500	3558	763	870	735
$Tm(OH)SO_4$	3502	3558	771	874	741
$Yb(OH)SO_4$	3504	3562	775	874	743

In some sulfate entities, two of the oxygen atoms, and in others, one of the oxygen atoms remain unlinked in an alternating manner. All other sulfate oxygen atoms are connected to the Ln-central atoms in the form of ordinary single coordinations. This rather loose arrangement of Ln-O coordination polyhedra, sulfate tetrahedra, and water molecules apparently prevents this crystal lattice from building up any noticeable tensions along the entire series of $Ln_2(SO_4)_3 \cdot 8H_2O$ compounds.[2,16]

Spectroscopic Studies

Vibrational Data. All $Ln(OH)SO_4$ complexes were characterized by FT-IR spectroscopy. As indicated in Table 3, two types of IR spectra were obtained for the two parts of this series. The first section with the lighter Ln-elements shows one O−H stretching mode between 3480 cm^{-1} and 3495 cm^{-1} respectively. The energies for this mode are in close proximity and show a slight incline in frequency for Eu and Gd. For the heavier $Ln(OH)SO_4$ complexes (Tb−Yb) one can observe a second O−H stretching mode. This fact corroborates very well with the X-ray structural data that clearly indicate that there are two crystallographic independent $Ln(OH)SO_4$ units from Tb-$(OH)SO_4$ throughout $Yb(OH)SO_4$.

The IR stretching frequencies for the first OH group (ν OH_I) continue a gradual increasing trend between 3495 cm^{-1} and 3505 cm^{-1}. The corresponding stretching frequencies of the second OH group (ν OH_{II}) can be found at somewhat higher energies between 3550 cm^{-1} and 3565 cm^{-1}. The non-equivalent Ln−OH distances of each $Ln(OH)SO_4$ species are represented by two O−H deformation modes between 730 cm^{-1} and 780 cm^{-1} (δ OH_I) and between 830 cm^{-1} and 880 cm^{-1} (δ $OH_{I'}$), throughout the entire series, as can be seen in Figure 8. Plotting the two sets of O−H deformation modes versus the decreasing ionic radius[15] correlates nicely with the structural analysis data. As bond lengths decrease with declining ionic radius the deformation vibrations of the OH groups become more restricted throughout the first section (Pr−Gd) of the series. This causes the deformation frequencies to incline gradually between the Pr and the Gd-hydroxysulfates. The rearrangement of the crystal lattice between Gd and Tb, and thereby, the reduction of the tensions, experienced by the crystal lattice, causes the deformation energies of both sets to be slightly lowered for the remaining lanthanide hydroxysulfates (Tb−Yb).

A gradual incline of the deformation frequencies can be observed for the remainder of the series starting with Tb at 744 cm^{-1} and 859 cm^{-1} (Figure 8). One would expect

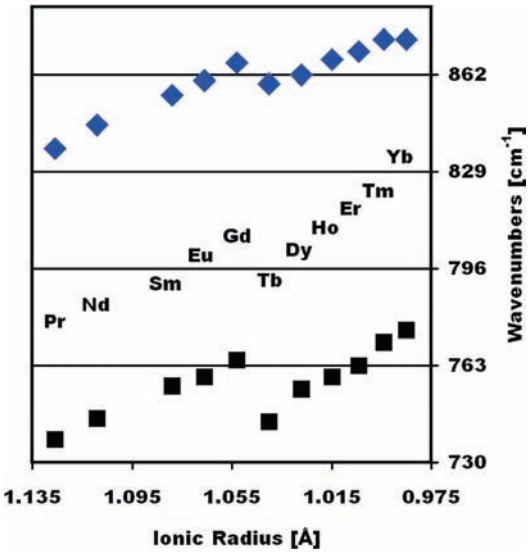

Figure 8. Correlation of the OH-I and OH-I′ deformation modes with decreasing ionic radius.[15] With declining ionic radius deformations become increasingly restricted, and as a result, the deformation modes continuously increase in energy. The deformation frequencies correlate well with the structural data, as a decrease in energy is observed for the deformation frequencies between Gd and Tb followed by a gradual increase throughout the remainder of the series.

two additional deformation bands for the heavier Ln-$(OH)SO_4$ compounds; however, only the lower frequency deformation band actually splits into two bands. The additional band can be observed between 720 cm^{-1} and 755 cm^{-1}. The higher energy deformation modes appear as one degenerate band.

These trends are illustrated in Figure 9, where we display the IR spectra of the Pr, Eu, and Tm-lanthanide hydroxysulfates. While the OH-stretching mode for Pr and Eu is represented by one band respectively at 3486 and 3488 cm^{-1}, the Tm-analogue, representing the heavier $Ln(OH)SO_4$, exhibits two separate bands correlating to the stretching modes ν OH_I and ν OH_{II}. Figure 9 demonstrates the O−H deformation modes to appear as two separate bands for Pr and Eu, while Tm is exhibiting a third separate band. The stretching modes of the sulfate groups can be found as three intense bands with more or less detailed substructures for the entire series of Ln-$(OH)SO_4$ complexes.

These bands represent the ν1 vibrational mode between 950 cm^{-1} and 1040 cm^{-1}, the ν3 vibrational mode between 1070 cm^{-1} and 1230 cm^{-1}, and the ν4 vibrational mode between 595 cm^{-1} and 660 cm^{-1}. For the Tb and Dy-species these bands appear as degenerate bands with no visual difference to the lighter analogues. From Ho on the second sulfate unit starts appearing as a more detailed substructure within all three major bands, which is represented by the IR spectrum of $Tm(OH)SO_4$ in Figure 9.

Conclusion

We applied a hydrothermal synthesis method utilizing similar conditions to produce an extended series of $Ln(OH)SO_4$ complexes at 170 °C. We synthesized the lanthanide hydroxysulfates from Pr through Yb, with the exception of Pm, applying the above-described method to obtain reproducible X-ray quality single crystals. Comparing the structural trends of these compounds throughout this series for the first time

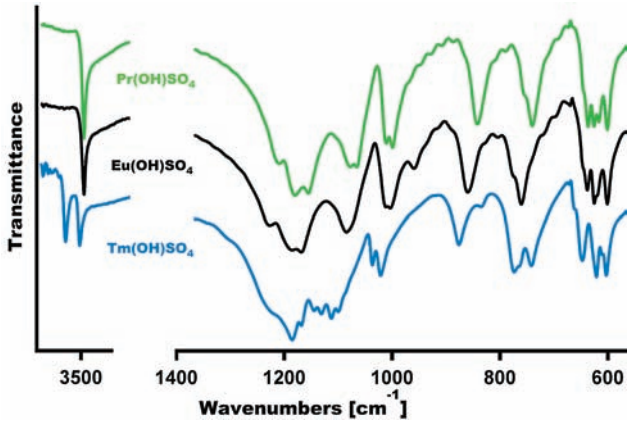

Figure 9. Selection of IR spectra showing the OH stretching and deformation modes of $Ln(OH)SO_4$, as well as various modes for the sulfate S−O bonds, in the order of decreasing ionic radius[15] with Ln = Pr, Eu, Tm.

provided us with an interesting insight into the properties of the resulting extended 3D lattices. Using the literature data previously published for the entire series of $Ln_2(SO_4)_3 \cdot 8H_2O$ compounds, as well as the data from our recent manuscript describing an extended series of $Ln(OH)_2Cl$ complexes, we were able to uncover some interesting trends. It appears that the crystal lattice with the highest level of rigidity exhibits the most drastic changes along these three Ln-element series to compensate for tension buildup caused by the decreasing Ln^{3+} ionic radius and the corresponding decline of the Ln-ligand bond distances. The $Ln_2(SO_4)_3 \cdot 8H_2O$ complexes, for instance, form open frameworks with 8-coordinate Ln-O polyhedra, in which the Ln-metal centers are linked by sulfate groups in a loose manner within 2D layers. Some of the sulfate oxygen atoms remain uncoordinated. Hydrogen bonds stemming from the water molecules tie these layers together along the "*a*" axis. As these frameworks possess a high level of flexibility, the resulting lattice structures do not experience any noticeable tension buildup along the entire series. Thus, the lattice does not respond with any significant structural adjustments. As a result, the lattice maintains the coordination number 8 while the unit cell parameters *a*, *b*, and *c* are showing a gradual decrease correlated to the declining ionic radius. At the same time the unit cell angle β does not change significantly.[2,16]

In contrast, the anhydrous $Ln(OH)_2Cl$ complexes assemble in a somewhat more rigid 3D extended lattice structure. Even though the coordination number 8 is maintained throughout the entire series and the unit cell parameters *b* and *c* show a gradual decrease as correlated to the ionic radius, cell parameter *a* shows some remarkable fluctuations along the series. The angle β declines significantly throughout this series, which results in significant tension buildup in the crystal lattice as ligand atoms close in on each other. The lattice seems to compensate for the strain buildup by adjusting the cell parameter *a* accordingly. As a result the unit cell volume gradually decreases while at the end of the series, the lattice actually recovers some volume space via the adjustments in "*a*" direction.[5]

The crystal lattice of the anhydrous $Ln(OH)SO_4$ complexes shows the highest level of rigidity and seems to alleviate the inclining strain along the series with significant rearrangements of the crystal structure between elements Gd and Tb, which goes along with a change of the coordination sphere. In the first part of this series (lighter Ln-elements), the rigid sulfate tetrahedra are three-dimensionally linked to six different metal centers, as opposed to the $Ln_2(SO_4)_3 \cdot 8H_2O$, in which two crystallographic different sulfate entities are linked to 2 and 3 metal centers via single Ln-O coordinations in only two dimensions. The lighter $Ln(OH)SO_4$ complexes between Pr and Gd (except Pm) are composed of LnO_9 polyhedra, in which the Ln-metal centers are two-dimensionally linked in the "*ac*" layer by hydroxy groups in μ^3 manner and by sulfate groups in μ^2 fashion as well as single coordinations. The sulfate groups tie the layers together along the "*b*" axis via a sixth regular coordination between one sulfate oxygen atom and one Ln-metal center. With lessening Ln^{3+} ionic radius along the series LnO_9 polyhedra are closing in, increasing the torque on the sulfate groups, which become more obstructed and seem to counteract this torque by exhibiting an inclining degree of torsion into the "*ac*" plane. We believe that the torsion of the sulfate entities allows the crystal lattice to compensate for some of the tensions caused by the declining ionic radius and bond distances. The unit cell volume gradually decreases, but apparently this response seems to be energetically favorable only up to $Gd(OH)SO_4$. From terbium on the strain placed on the crystal lattice elevates the energy profile to unfavorable levels. The crystal lattice responds by reducing the coordination number from 9 to 8 and by restructuring the coordination sphere, which seems to offer an energetically more efficient structural arrangement. This causes the unit cell to gain sufficient volume for the remaining heavier $Ln(OH)SO_4$ complexes, which enables them to arrange in an isostructural manner between Tb and Yb. On the basis of the data for the yttrium analogue, we predict that this arrangement will most likely be similar for the Lu−counterpart.

We recorded the FT-IR spectra for the compounds investigated and believe that they represent the described structural changes very well. The O−H deformation modes show a gradual increase in energy for the first section of the series, and then readjust to lower energies for the second section, followed by another gradual increase throughout the remainder of the series. This matches the crystallographic trends very well and is in reconciliation with the decreasing bond lengths along the series.

We plan to investigate additional purely inorganic lanthanide mixed ligand compounds to further this knowledge.

Acknowledgment. This work was supported at the University of Louisiana at Monroe by the Department of Chemistry. We would like to thank the Louisiana Board of Regents for the sponsorship of this research under contract no. LEQSF(2007-10)-RD-A-40. Funding for the X-ray diffractometer at Youngstown State University was provided by NSF Grant 0087210, Ohio Board of Regents Grant CAP-491, and by Youngstown State University. The purchase of the X-ray diffractometer at Louisiana State University was made possible by Grant LEQSF(1999-2000)-ENH-TR-13, administered by the Louisiana Board of Regents. We also thank Dr. Brian Scott for some preliminary X-ray single crystal structural data that he obtained at the Los Alamos National Laboratory, Los Alamos, New Mexico.

Supporting Information Available: Crystallographic data in CIF format. Further details are given in Figures S1−S5. This material is available free of charge via the Internet at http://pubs.acs.org.